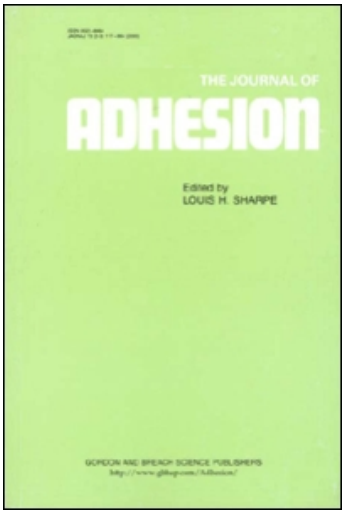

The Journal of Adhesion

Publication details, including instructions for authors and subscription information:
http://www.informaworld.com/smpp/title~content=t713453635

Peel Analysis Using the Finite Element Method

A. D. Crocombe[a]; R. D. Adams[a]
[a] Department of Mechanical Engineering, University of Bristol, Bristol, England

To cite this Article Crocombe, A. D. and Adams, R. D.(1981) 'Peel Analysis Using the Finite Element Method', The Journal of Adhesion, 12: 2, 127 — 139
To link to this Article: DOI: 10.1080/00218468108071194
URL: http://dx.doi.org/10.1080/00218468108071194

J. Adhesion, 1981, Vol. 12, pp. 127–139
0021–8464/81/1202–0127 $06.50/0

Printed in Great Britain

Peel Analysis Using the Finite Element Method

A. D. CROCOMBE and R. D. ADAMS
Department of Mechanical Engineering, University of Bristol, Bristol BS8 1TR, England

(*Received November 11, in final form November 27, 1980*)

Large displacement finite element analysis and subsequent experimental work has been used to investigate the adhesive peel test; at this stage, only elastic behaviour has been considered.

Both non-cracked and cracked configurations have been analysed, representing initial and continuous failure of the peel test. Analysis of the former indicated that initial failure was caused by the adhesive principal stresses driving a crack towards the interface with the flexible adherend. Investigation of the cracked configuration has shown that the amount of mode II loading at the crack tip is significant and is essentially independent of peel angle, load and adhesive or adherend modulus, only decreasing as the adhesive becomes incompressible. Failure (propagation) has been shown to occur at a critical applied bending moment for a particular adherend and adhesive, independent of peel angle. Further, the strength (load) measured by the peel test is not proportional to the actual strength of the adhesive, a small increase in the adhesive strength causing a much larger increase in the applied peel load.

INTRODUCTION

The adhesive peel test exists in a number of forms such as the stripping, "**T**", floating roller and climbing drum tests. These are all essentially variations of a common theme, shown schematically in Figure 1. A peel load is applied at some angle to the adhesive through a flexible adherend. This tests the adhesive in its weakest mode, since strengths from shear lap tests are many times greater than those from peel tests even for high peel strength adhesives. This is because the load, P, and more importantly, the bending moment, M, due to the moment of the load about the bond end (see Figure 1) are reacted over a very small region of the adhesive at the bond end, thus causing high local stresses.

The various peel tests have only been used in a comparative manner, largely because of the lack of information about the adhesive stress distribution. Further, small modifications of adhesive structure, such as adding

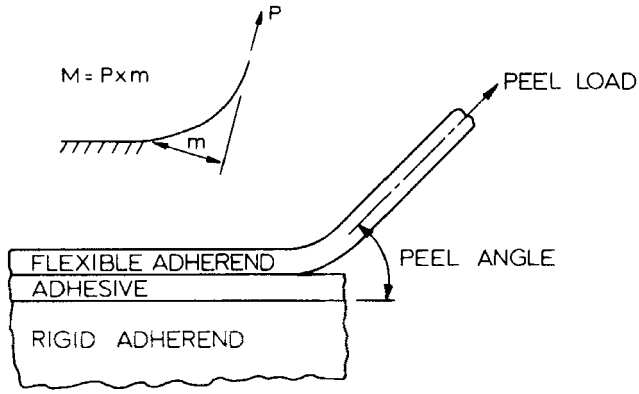

FIGURE 1 Schematic representation of the peel test.

second phase elastomeric components, can drastically increase peel strength but with only minimal effects on lap shear strength. The purpose of this work was therefore to investigate the mechanics of the peel test in order to establish the way in which such joints fail. This necessitates the evaluation of the adhesive stress distribution in the peel test and subsequent application of a failure criterion based on fracture mechanics concepts. The finite element technique, which has already been used successfully for the analysis of adhesive joints,[1] has been used here. This technique provides a method of stress analysis for geometrically complicated structures. The effects of plasticity may well be important but, at this stage, elastic behaviour has been assumed.

Previously, the peel test has been represented either by a non-cracked, bi-material model or by a cracked, single-material model. Among the workers who adopt the first approach are Kaelble[2] and Nicholson.[3] They have modelled the adhesive as a layer of tension and shear springs and assume failure at a maximum stress.

Anderson *et al.*[4] and Kendall[5] have adopted the second approach, determining the load required for propagation by applying an energy balance to the system in an attempt to quantify peel failure. However, these analyses cannot consider mixed mode fracture and are only a simplified model of the real bi-material test.

APPLICATION OF FRACTURE MECHANICS TO BI-MATERIAL SYSTEMS

In applying fracture mechanics principles to bi-material systems, some workers, such as Gledhill *et al.*,[6] have followed the traditional approach,

considering cohesive fracture of the adhesive. Others, such as Anderson *et al.*,[7] have analysed interfacial fracture of bi-material systems, using an interfacial fracture energy (γ_a) term in place of the usual cohesive fracture energy (γ) term. Although interfacial fracture energy is not strictly a material property, it can be considered as a parameter in a continuum sense, and defines the amount of energy required to break interfacial bonds.

As the locus of failure in the peel test is either interfacial between the adhesive and the flexible adherend, or cohesive extremely close to the flexible adherend, the interfacial approach has been used.

Analysis for interfacial fracture is similar to that for cohesive fracture. This fracture may be considered in two parts: the first, called mode I in fracture mechanics terminology, involves cleavage (tensile) failure and the second, mode II, involves shear failure. Practical situations usually consist of a combination of both modes.

Basically, the crack is assumed to propagate only if the energy released on propagation is sufficient to break the interfacial bonds. This critical energy level is a function of the mode I and II interfacial fracture energies, γ_{aI} and γ_{aII}, the energies required to separate a unit area of two materials subjected to pure mode I and mode II loading respectively. The proportions of each are determined by the amount of that mode present at the crack tip. As γ_{aII} can be more than twice γ_{aI},[4] a knowledge of the relative amounts of mode I and II present is essential, and it was an objective of this work to investigate this relationship in various configurations of the peel test. This has been achieved by using the finite element method to investigate the stress field around the crack tip.

In cohesive linear fracture, the stresses around the crack tip can be written as (Paris and Sih[8])

$$\sigma_i = K_i F(\theta)/(2\pi r)^{1/2}$$

where r and θ are polar co-ordinates with the origin at the crack tip. The stress intensity factor (K_i) can be used to determine the proportion of modes I and II loading present at the crack tip.

In bi-material systems, a similar form for the stresses is found.[7] Thus, in the analysis of the peel test with a crack already present a general relationship for the stresses on the interface will be assumed in the form

$$\sigma_i = C_i/r^{1/2}$$

where C_i is the intensity of the singularity. The value of C_i, which gives a measure of the ith mode present at the crack tip, can be obtained from the stress field around the crack tip.

Two general comments on this approach should be made. First, the effects of plasticity are not included at this stage. However, in practice, the interfacial

fracture energy terms will include some of these effects and careful choice of adherend and adhesive will minimise any remaining errors. Second, this approach is equally applicable if the fracture is cohesive, the values of cohesive fracture energy of the adhesive, γ, replacing the interfacial fracture energy, γ_a.

THE FINITE ELEMENT PROCEDURE

This technique has been used successfully many times in uncracked bi-material systems. Trantina[9] and Wang[10] have extended the technique to investigate cohesive fracture of an adhesive layer in a bi-material system, while Anderson *et al.*[7] and Lin[11] considered interfacial fracture of a bi-material system. In the present work, the cracked peel test is modelled as interfacial fracture in a bi-material system and the finite element technique is used to obtain the stress distributions around the crack tip and hence the intensities C_1 and C_2 introduced earlier. The four elements adjacent to the crack tip have their mid-nodes distorted, after Henshall and Shaw,[12] to produce the appropriate crack tip singularity.

As a result of the large rotation present in the peel test, the assumptions of small displacement theory (upon which most finite element codes are based) do not apply and the strain-displacement relationship is no longer linear. If the strains can still be considered as small, then the governing equation is found to be[13]

$$2\varepsilon_{pq} = \frac{\partial D_p}{\partial q} + \frac{\partial D_q}{\partial p} + \left[\frac{\partial \mathbf{D}}{\partial p} \cdot \frac{\partial \mathbf{D}}{\partial q}\right] \text{where } p, q = x, y, z$$

where $\mathbf{D} = \mathbf{u} + \mathbf{v} + \mathbf{w}$ (the displacement vector).

Direct solution of the finite element formulations is no longer possible, because of the non-linear nature of the governing equations, and a solution has to be achieved using an iterative scheme, testing the solution at each step for convergence. A detailed description of large displacement finite element formulations is given elsewhere.[14]

A large displacement finite element program, outlined above, was written which incorporated both triangular and quadrilateral quadratic isoparametric elements. The quadrilateral elements are good general purpose elements and have been used successfully by many workers. The triangular elements have been included to allow local mesh refinement, and a local refinement block has been used to introduce extra elements locally around the crack tip, shown in Figure 2, including the crack tip elements mentioned earlier. A mesh generating routine has been written which incorporates the previous two features.

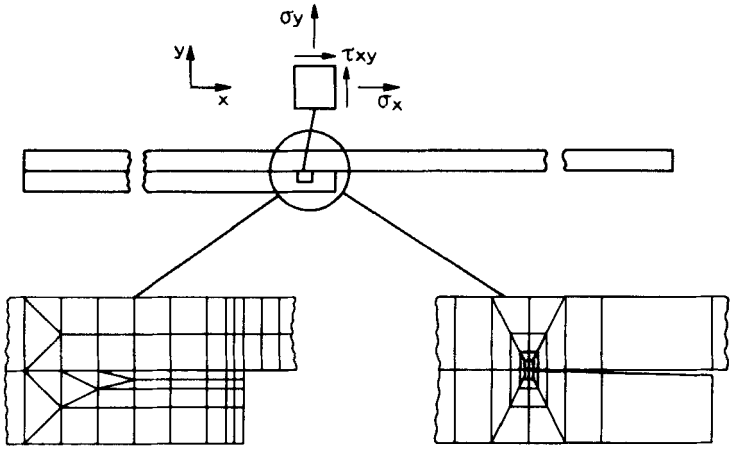

FIGURE 2 Finite element meshes used in the analysis of the non-cracked and cracked peel tests.

ANALYTICAL RESULTS

The peel test configuration has been modelled both as a cracked and as a non-cracked bi-material system. Where the system contains a crack, it is modelled by giving the adhesive and adherend separate nodes on the interface. The rigid substrate is represented by constraining the appropriate adhesive nodes in both directions. Initial analyses considered variations in nominal peel angle, ω (90, 60 and 30 degrees) and peel load, P (1.0, 0.5 and 0.1 Nmm^{-1}). These were then extended to include a range of adhesive and adherend properties. Specific details of the initial analyses are given in Table I. The free length of the adherend was chosen so that the difference between the slope at the end of the adherend (calculated using large displacement beam theory) and the nominal peel angle was no more than 0.05°. This resulted in a maximum length of 220 mm ($P = 0.1$ Nmm^{-1}, $\omega = 90°$) and a minimum length of 30 mm ($P = 0.5$ Nmm^{-1}, $\omega = 30°$).

TABLE I

Adhesive and adherend details in initial analyses

Parameter	Adhesive	Adherend
Tensile modulus (GNm^{-2})	2.8	210.0
Poisson's ratio	0.4	0.3
Thickness (mm)	0.2	0.2

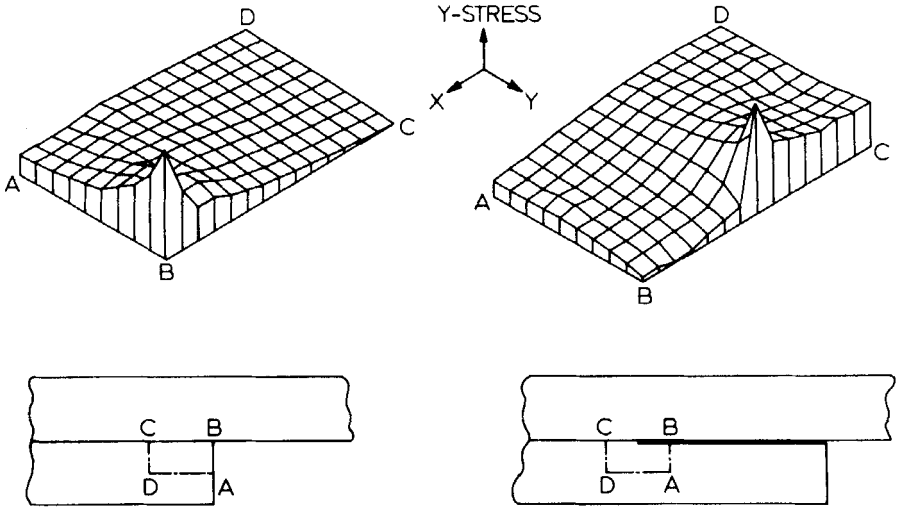

FIGURE 3 Adhesive transverse direct stress fields in the non-cracked and cracked peel tests.

The finite element meshes were refined locally until negligible change in the stress distributions was obtained. The meshes used for the cracked and non-cracked configurations followed the same pattern, the adhesive and the adherend being modelled by coarse elements (10 mm × 0.2 mm) for most of the structure, reducing to the refined meshes shown in Figure 2. The smallest elements were 0.0125 mm × 0.025 mm in the cracked configuration and 0.025 mm × 0.025 mm in the non-cracked system.

Figure 3 gives a general picture of the adhesive stress distribution in both the non-cracked and cracked configurations. The adhesive transverse direct stress (σ_y) is shown in an isometric projection. The base of the projection refers to an area of the adhesive normal to the plane of the crack and the height is the stress level. A singularity which lies on the interface exists in both cases, either at the bond end, or at the crack tip. The stress on the free surface of the crack, which should be zero, fluctuates about this value because the surface stresses are obtained by extrapolation from the integration (Gauss) points within the element.

INVESTIGATION OF THE NON-CRACKED SYSTEM

Comparison between the adhesive transverse direct stress (σ_y) distribution resulting from the finite element analysis and the analysis of Kaelble[2] is shown in Figure 4. The solid curve is from Kaelble and the discrete points from the

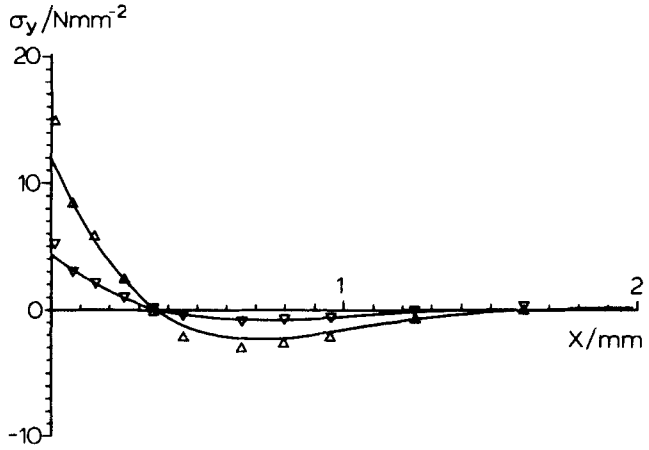

FIGURE 4 Variation of adhesive transverse direct stress, σ^y, with distance, x, from the bond end in the non-cracked peel test. △, 90° peel test; ▽,30° peel test.

finite element analysis. Kaelble assumes the stress across the adhesive thickness is constant, but Figure 3 clearly shows that this is not so. Such an approach grossly underestimates the value of the maximum stress, only providing an average stress. However, to make a comparison, the finite element stresses have been averaged across the adhesive thickness. Close agreement was then found for the complete range of peel loads and angles considered.

Figure 5 shows details of the principal stresses in the adhesive, indicating that the maximum stress occurs at the bond end adjacent to the flexible adherend. Assuming that failure occurs when this maximum stress reaches a

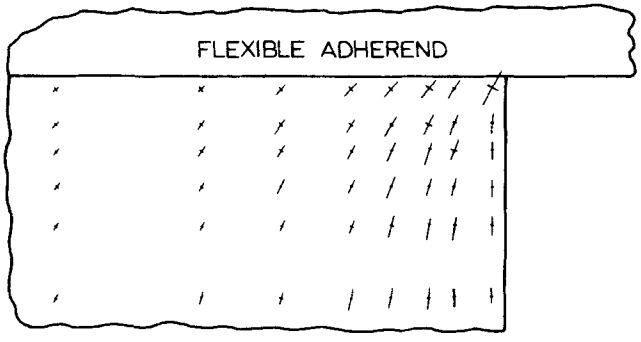

FIGURE 5 Distribution of the adhesive principal stresses in the non-cracked peel test. The principal stresses are shown as line vectors.

certain level, it can be seen that a crack will be driven towards the interface with the flexible adherend, as is found in practice. The plot shown is for a 90° peel test, but it is characteristic of the other peel angles and load cases investigated.

INVESTIGATION OF THE CRACKED SYSTEM

The main purpose of this section of the analysis was to determine the intensities, C_i, for the adhesive transverse direct stress (σ_y) and shear stress (τ_{xy}) along the interface, and hence the proportions of modes I and II loading present at the crack tip. The singular relationships for both stresses, as discussed earlier, were assumed to be given by

$$\sigma_i = C_i/r^{1/2}$$

and the intensities were calculated by evaluation at points close to the crack tip using the relationship above and extrapolation of these values to the crack tip, this being a familiar method in linear elastic fracture mechanics.

The results obtained are shown in Table II, the superscript * referring to the 90° peel test.

TABLE II

Adhesive intensity factors for the cracked peel test

Configuration	Proportion mode II $C_{II}/(C_I+C_{II})$	Mode I intensity C_I/C_I^*	Applied moment M/M^*
90° ($P = 0.5$ Nmm^{-1})	29%	1	1
60° ($P = 0.5$ Nmm^{-1})	30%	0.72	0.70
30° ($P = 0.5$ Nmm^{-1})	30%	0.36	0.34
90° ($P = 1.0$ Nmm^{-1})	29%	1.37	1.40
90° ($P = 0.1$ Nmm^{-1})	30%	0.47	0.46

$C_I^* = 26.77$ Nmm$^{-3/2}$

The proportion of mode II loading at the crack has been found to be essentially independent of peel angle and load for the range of parameters investigated. This is because the adhesive stresses are caused mainly by bending and not by direct loading in the adherend. This has been demonstrated by showing that the intensities are proportional to the bending moment (compare the last two columns of Table II).

Failure in the peel test at a critical intensity therefore implies failure at a critical bending moment. Thus, for a particular adherend and adhesive, failure should occur at a constant bending moment independent of peel

TABLE III

Variation of mode II loading in the cracked peel test with adhesive and adherend properties

Change in material property	Proportion Mode II $C_{II}/(C_I + C_{II})$
Initial analysis (Table I)	29%
Adhesive modulus = 5.0 GNm^{-2}	31%
Adhesive modulus = 0.5 GNm^{-2}	25%
Adherend modulus = 70.0 GNm^{-2}	32%
Adhesive Poisson's ratio = 0.3	28%
Adhesive Poisson's ratio = 0.49	12%

angle. Using large displacement theory, the bending moment, M, applied to the peel test can be expressed in terms of the load, P, and the peel angle, ϕ,[2] as

$$M = [2EIP(1-\cos\phi)]^{1/2},$$

where EI is the flexural rigidity of the material. Thus, the stresses, which are proportional to the bending moment, are proportional to the square root of the load. This illustrates the non-linear nature of the peel test, that is, a small increase in adhesive strength causes a much larger increase in the load required to cause failure of the peel test (seen in columns 1 and 3 of Table II). In fact the stresses are not exactly proportional to the square root of the load, since the above expression for the bending moment neglects deflections in the bonded region of the peel test, which causes higher bending moments than are actually present; this effect is worse at higher loads.

The variation of mode II loading present with different adhesive and adherend materials was investigated by changing the appropriate property in the analysis from that outlined earlier. The results are shown in Table III.

It can be seen that the amount of mode II is largely independent of either adhesive or adherend tensile modulus and only decreases significantly as the adhesive becomes incompressible (that is as Poisson's ratio tends to 0.5).

EXPERIMENTAL RESULTS

The peel testing apparatus is shown schematically in Figure 6. The peel angle is set by rotating the carrier plate and the specimen peeled by the upward movement of the crosshead. Since the horizontal distance between the crack tip and the grips on the load cell is known together with the applied load then, by using large displacement beam theory, the actual peel angle can be evaluated (Appendix 1).

To avoid plastic deformation in the adherend, thin, spring steel strips

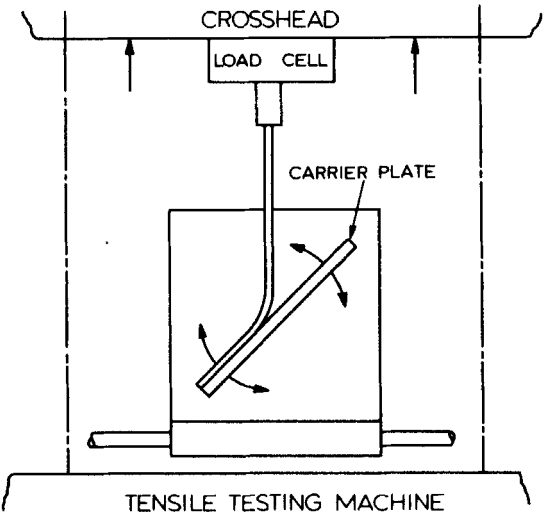

FIGURE 6 Schematic representation of the peel test apparatus.

(0.12 mm thick) were used as the flexible adherend, a thicker steel section being used for the rigid base. Both adherends were de-greased, abraded with a fine sand blast, re-cleaned and bonded with a high peel strength adhesive.

Plots of peel load and peeled distance were made and two data points were taken from each test, one at the beginning and one at the end. The results are shown in Figure 7. Also shown in Figure 7 is a solid line which is a constant bending moment curve with a least squares fit to the data. The form of this curve is obtained from the expression for the bending moment outlined earlier and found in.[2] The points lie close to this curve, indicating that failure does occur at a constant bending moment, as predicted by the finite element analysis.

CONCLUSIONS

An elastic large displacement finite element analysis of the peel test and subsequent experimental work has revealed a number of important points.

Firstly, initial failure is caused by the adhesive principal stresses driving a crack towards the interface with the flexible adherend.

Secondly, for a particular adherend and adhesive, failure will occur at a critical applied bending moment independent of peel angle. Further, the peel test has been shown to be non-linear with load, that is the actual adhesive strength is essentially proportional to the square root of the peel load.

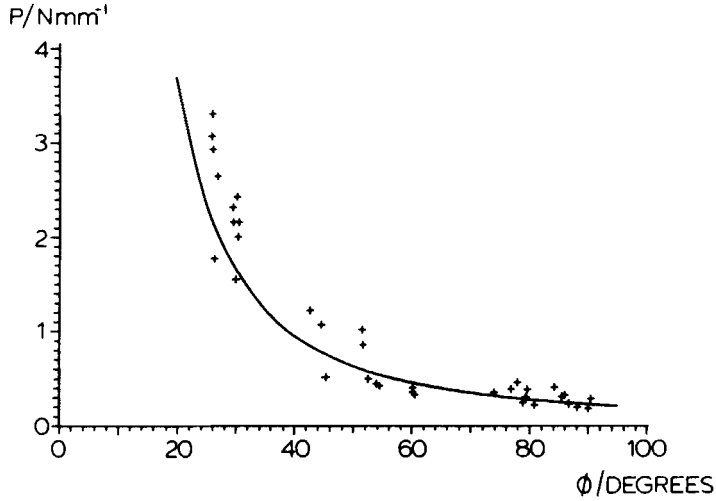

FIGURE 7 Variation of peel load, P, with peel angle, ϕ. The solid curve is a line of constant bending moment with a least squares fit to the experimental points.

Finally, the proportion of mode II loading at the crack tip has been shown to be essentially independent of the peel load and angle, and the adhesive or adherend modulus. The proportion is significant, about 30%, decreasing to less than half of this value as the adhesive becomes incompressible. This last point provides the information required for a fracture mechanics analysis based on the interfacial fracture energy approach outlined earlier.

This work has been carried out for an elastic system. However, the effects of plastic behaviour of both the adherend and the adhesive can be assessed by evaluating the energy required for the plastic deformation of the materials. In an attempt to establish this, the authors are currently undertaking an elasto-plastic large displacement finite element analysis of the peel test and these results will be reported later.

APPENDIX I

Determination of Actual Angle of Peel, ϕ

Definition of variables:

ω = nominal peel angle

$\phi = \omega - \alpha$ = actual peel angle

s = length of bent portion of strip.

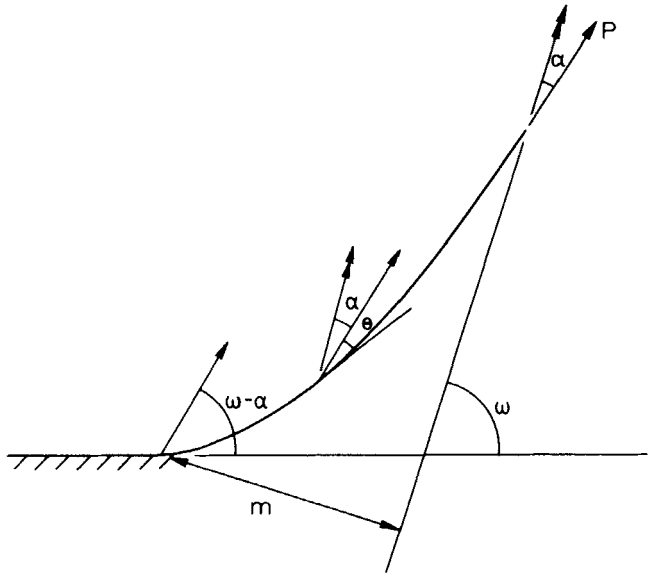

FIGURE 8 Definition of variables used in the evaluation of the actual angle of peel.

From[2] and with reference to Figure 8:

$$d\theta/ds = [2P(1-\cos\theta)/EI]^{1/2} \tag{a}$$

$$\therefore (2P/EI)^{1/2}\int_0^s ds = \int_0^{\omega-\alpha}(1-\cos\theta)^{-1/2}d\theta$$

Evaluating the integrals leads to:

$$(P/EI)^{1/2}s = [\ln(\tan(\theta/4))]_0^{\omega-\alpha} \tag{b}$$

For the bent portion of the strip, Figure 8:

$$dm/ds = \sin(\theta+\alpha) \tag{c}$$

Substituting (c) in (a)

$$\sin(\theta+\alpha)\,d\theta/dm = [2P(1-\cos\theta)/EI]^{1/2}$$

$$\therefore (2P/EI)^{1/2}\int_0^m dm = \int_0^{\omega-\alpha}\sin(\theta+\alpha)(1-\cos\theta)^{-1/2}\,d\theta$$

Evaluating the integrals leads to:

$$(P/EI)^{1/2}m = 2[\sin(\theta/2+\alpha)+\sin\alpha[\ln(\tan\theta/4)]/2]_0^{\omega-\alpha} \tag{d}$$

Substituting (b) in (d) gives

$$(P/EI)^{1/2}m = 2\sin((\omega+\alpha)/2)+\sin\alpha((P/EI)^{1/2}s-2) \quad \text{(e)}$$

Equation (e) forms the basis for an iterative scheme to calculate α, knowing P, E, I, m, s and ω, *viz.*:

$$\alpha_i = \sin^{-1}[((P/EI)^{1/2}m-2\sin((\omega+\alpha_{i-1})/2))/((P/EI)^{1/2}s-2)]$$

where $\alpha_0 = 0$.

References

1. R. D. Adams and N. A. Peppiatt, *J. Strain Anal.* **9,** 185 (1974).
2. D. H. Kaelble, *Trans. Soc. Rheology* **IV,** 45 (1960).
3. D. W. Nicholson, *Int. J. Fract.* **13,** 279 (1977).
4. G. P. Anderson, K. L. DeVries and M. L. Williams, *Exp. Mech.* **24,** 11 (1976).
5. K. Kendall, *J. Adhesion* **5,** 179 (1973).
6. R. A. Gledhill *et al.*, *Polymer* **19,** 574 (1978).
7. G. P. Anderson, K. L. DeVries and M. L. Williams, *Int. J. Fract.* **9,** 421 (1973).
8. P. C. Paris and G. C. Sih, *Amer. Soc. for Testing and Matls. Special Tech. Pub. No. 381* (ASTM, Philadelphia, 1965), p. 30 (1965).
9. G. G. Trantina, *J. Comp. Maths.***6,** 192 (1972).
10. S. S. Wang, J. F. Mandell and F. J. McGarry, *Research Report R76–1*, Dept. of Matls. Sci. & Eng., Mass. Inst. of Tech., "Fracture of Adhesive Joints" (1976).
11. K. Y. Lin and J. W. Mar, *Int. J. Fract.* **12,** 521 (1976).
12. R. D. Henshell and K. G. Shaw, *Int. J. Num. Methods in Eng.* **9,** 495 (1975).
13. H. C. Martin, *NASA, Technical Report No. 32–931*, "Large Deflection and Stability Analysis by the Direct Stiffness Method", (1966).
14. G. C. Nayak, *Ph.D. Thesis*, Univ. of Wales (1971).